Dang-Gui-Si-Ni decoction facilitates wound healing in diabetic foot ulcers by regulating expression of AGEs/RAGE/TGF-β/Smad2/3

Shuyang Zhang

zsyzsy0522@163.com

Shaoxing Hospital of Traditional Chinese Medicine (Shaoxing TCM Hospital Affiliated to Zhejiang Chinese Medical University)

Yanwen Xu

Affiliated Hangzhou First People's Hospital, School of Medicine, Westlake University

Chenyang Zhang junior

Xiangya School of Medicine，Central South University

Xiao Chen

Shaoxing Hospital of Traditional Chinese Medicine (Shaoxing TCM Hospital Affiliated to Zhejiang Chinese Medical University)

Jiayan Zhu

Shaoxing Hospital of Traditional Chinese Medicine (Shaoxing TCM Hospital Affiliated to Zhejiang Chinese Medical University)

Research Article

Keywords: Diabetic foot ulcer, Dang-Gui-Si-Ni decoction, TGF-β, Smad2/3, Angiogenes

Posted Date: May 2nd, 2024

DOI: https://doi.org/10.21203/rs.3.rs-4323205/v1

Additional Declarations: No competing interests reported.

Abstract

Purpose

Diabetic foot ulcer (DFU) is a predominant complication of diabetes mellitus with poor prognosis accompanied by high amputation and mortality rates. Dang-Gui-Si-Ni decoction (DSD), as a classic formula with a long history in China, has been found to improve DFU symptoms. However, mechanism of DSD for DFU therapy remains unclear with no systematic elaboration.

Methods

In vivo, following establishment of DFU rat model, DSD intervention with low, medium and high doses was done, with Metformin (DM) as a positive control group. With wound healing detection, pathological changes by HE staining, inflammatory factor expression by ELISA and qRT-PCR, oxidative stress levels by ELISA, and AGEs/RAGE/TGF-β/Smad2/3 expression by Western blot were performed. In vitro, intervention with LY2109761 (TGF-β pathway inhibitor) based on DSD treatment in human dermal fibroblast-adult (HDF-a) cells was made. Cell viability by CCK8, migration ability by cell scratch, apoptosis by flow cytometry, and AGEs/RAGE/TGF-β/Smad2/3 expression by Western blot were measured.

Results

DFU rats exhibited elevated AGEs/RAGE expression, whereas decreased TGF-β1 and p-Smad3/Smad3 protein expression, accompanied by higher IL-1β, IL-6, TNF-α levels, and oxidative stress. DSD intervention reversed above effects. Glucose induction caused lower cell viability, migration, TGF-β1 and p-Smad3/Smad3 protein expression, with increased apoptosis and AGEs/RAGE expression in HDF-a cells. These effects were reversed after DSD intervention, and further LY2109761 intervention inhibited DSD effects in cells.

Conclusion

DSD intervention may facilitates wound healing in diabetic foot ulcers by regulating expression of AGEs/RAGE/TGF-β/Smad2/3, providing scientific experimental evidence for DSD clinical application for DFU therapy.

Introduction

Diabetic foot ulcers (DFU), considered a major clinical issue in diabetic complications, is essentially recognized as chronic and non-healing wounds that primarily result from the presence of diabetic neuropathy, vascular disease, and bacterial infection[1]. Affecting estimated 18.6 million individuals globally each year, DFU is strongly correlated to an increase in amputation and mortality rates[2]. Of

these, approximately 19–34% of diabetic patients experienced foot ulcers or tissue necrosis[3]. The ulcer and amputation rates of Chinese diabetic patients were 8.1% and 5.1% per year, respectively[4]. Undoubtedly, diabetic foot therapy involves extremely high costs as well as physical pain and psychological burdens, resulting in severe family, social, and economic impacts[5]. Given urgency of the situation, there is an immediate need to enhance clinical focus on DFU prevention and therapy.

First mentioned in the *Treatise on Febrile Diseases*, Dang-Gui-Si-Ni (DSD) decoction exists thousands of years of application in Chinese medicine clinical practice to date[6][6]. Known as one of the top 100 classical Chinese medicine prescriptions, composition of DSD decoction contains seven herbs, including *Angelica sinensis* (Oliv.) Diels, *Cinnamomum cassia* (L.) D. Don, *Asarum heterotropoides* F. Schmidt, *Paeonia lactiflora* Pall., *Glycyrrhiza* uralensis Fisch., *Cyperus papyrus L.*, and *Ziziphus jujuba* var. spinosa (Bunge) Hu ex H.F.Chow. [7] [7]. It was confirmed that DSD possessed pharmacological effects such as vasodilatation, antioxidant, anti-inflammatory and antinociception[8, 9]. Furthermore, a protective effect of DSD against hypoxic injury of pancreatic islet endothelial cells and diabetic peripheral neuropathy has been demonstrated[7, 9]. You *et al.*[10] conducted a randomized controlled trial applying modified DSD decoction, and found that modified DSD decoction led to improvement on clinical symptoms of DFU patients, with therapeutic effects on diabetic-complicated vascular disease. However, underlying mechanisms of DSD for DFU therapy remain to be unclearly and unsystematically elaborated.

Studies have demonstrated that persistent hyperglycemia-induced neuropathy (pudendal nerve damage), vasculopathy, persistent infections, and excessive inflammation underlie the onset and progression of DFU[1]. DFU contributed to development of excessive oxidative stress, which in turn leading to inflammatory response, MI/M2 macrophage imbalance, and impaired proliferation and differentiation of fibroblasts[11]. It was proved that vascular endothelial growth factor (VEGF) and TGF-β1 expression exhibited decreased in DFU models, with increased apoptosis and decreased cell proliferation and migration, thereby hindering wound healing[12]. Shi *et al.*[13] identified that restoration of TGF-β1/Smad pathway-mediated autophagy in epidermal cells made promotion of diabetic wound healing. Moreover, over-activation of AGEs-RAGE pathway likewise further aggravated DFU injuries[11]. The bitter melon extract was evidenced to improve wound healing by inhibition of AGEs-RAGE pathway, which in turn facilitated angiogenesis in diabetic wounds[14]. Targeting AGEs-RAGE pathway holds great potential for DFU therapy. With combining network pharmacology, molecular docking and meta-analysis, a latest study revealed that DSD may exert its therapeutic effects on DFU through regulation of cell proliferation, inflammatory response, oxidative stress and angiogenesis promotion via AGE-RAGE pathway[15][15]. In particular, molecular docking results demonstrated best docking between DSD and VEGF, further concluding that VEGF was probably to be the target protein of DSD for DFU treatment, thereby lowering IL-6 and TNF-α levels, inhibiting inflammation, and enhancing wound healing[15][15]. Additionally, Danggui Buxue decoction, containing *Angelicae sinensis* radix and *Astragali* radix, may function as a therapeutic agent for diabetic interstitial fibrosis rats by TGF-β1/Smads pathway[16], with a network pharmacology analysis finding of improvement on diabetic nephropathy with AGEs-RAGE pathway[17] [17]. Considering all above findings and conclusions, it was reasonable to make an inference that TGF-β1/Smads/AGE/RAGE expression took an important role in DSD treatment of DFU.

Therefore, we performed the establishment of DFU rat model and high glucose-induced cellular model to complete investigation of therapeutic effects and mechanisms of DSD on DFU mediated by TGF-β1/Smads/AGE/RAGE expression. The present study offered prospective therapeutic targets for DFU therapy as well as scientific experimental evidence for DSD clinical application as a promising treatment for DFU, broadening new avenues for DFU trauma treatment.

Materials and methods

Preparation of Dang-Gui-Si-Ni (DSD) decoction

According to Zhongjing Zhang's Treatise on Febrile Diseases, composition of DSD was displayed as Table 1. We completed the extraction by referring to the previous research[8][8]. Following distilled water extraction and filtration, a stock solution of 1.0 g/mL was obtained and stored frozen.

Table 1
Composition of DSD

Scientific name	Chinese pinyin name	Weight (g)
Angelica sinensis (Oliv.) Diels	Danggui	9
Cinnamomum cassia (L.) D. Don	Guipi	9
Asarum heterotropoides F. Schmidt	Xixin	9
Paeonia lactiflora Pall.	Shaoyao	9
Glycyrrhiza uralensis Fisch.	Gancao	6
Cyperus papyrus L.	Zhicao	6
Ziziphus jujuba var. spinosa (Bunge) Hu ex H.F.Chow.	Suanzao	12
Notes:		

Abbreviations: DSD, Dang-Gui-Si-Ni decoction.

Animals

Forty-ejght healthy male Sprague-Dawley (SD) rats, with body weight of approximately 200 g, were purchased from Shanghai SLAC Laboratory Animal Co.,Ltd (license number: SCXK (Hu) 2022-0004). Subsequently, these rats were housed in Zhejiang Eyong Pharmaceutical R&D Co., Ltd (license number: SYXK (Zhe) 2023-0027) at 22 ± 2°C temperature, 50%-60% humidity, and a light/dark cycle of 12 h. All rats got free access for water and food.

Construction of rat diabetic foot ulcer (DFU) models

Diabetic rat modeling[18]: The provision of a high-fat diet (58% fat, 25% protein, 17% carbohydrate) was carried out to build up insulin resistance for 8 weeks. After 15 h fasting, intraperitoneal injection of 1% streptozotocin (STZ, 50 mg/kg) was done for diabetic rat model development. Tail vein blood was collected on the 3rd and 7th d after injection, respectively, and detection of fasting blood glucose (FBG) was made with a glucometer. Successful diabetic rat modeling was represented by blood glucose greater than or equal to 16.7 mmol/L, and typical symptoms of polydipsia, increased appetite, polyuria, and emaciation[19][19].

Subsequent DFU modeling[12]: Following mild anesthesia with 3% isoflurane for rats, skin on the back of feet was depilated, as well as ensuring no death due to hypothermia. Saline cleansing was done and then sterilization operation with iodophor and 75% medical alcohol cotton balls was repeated several times. Afterwards, we placed a prepared 5 mm × 5 mm square plastic sheet on the dorsum of rat feet and marked it with a black marker with lines. The cut of skin was conducted along the markings with surgical scissors, with all wounds deep enough to reach the fascial layer in order to prepare a 5 mm × 5 mm wound. The exposure was maintained throughout after completion of hemostasis and sterilization.

Experiment design

Thirty-six rats were classified randomly into 6 groups (n = 6): Sham group, DFU group, DFU + metformin (DM) group, DFU + low dose of DSD (DSD-L) group, DFU + medium dose of DSD (DSD-M) group, and DFU + high dose of DSD (DSD-H) group. The rats in Sham group were treated with a normal diet, with open wounds similarly constructed. The medication was starting on the day of successful DFU modeling. We performed calculations based on the 0.018 conversion factor of body surface area conversion factor for rats (200 g) and humans (70 kg), where the DSD-M group (5.4 g/kg/d) was the corresponding clinical dose[20][20]. The doses of DSD-L group and DSD-H group were 2.7 g/kg/d and 10.8 g/kg/d, respectively, in reference to previous study[20][20]. The Sham group and DFU group were gavaged with distilled water (10 mL/kg). Administration was done by gavage once daily for 21 d. On day 22, euthanasia of rats were made by CO_2 inhalation, and collection of samples was performed for subsequent tests.

Wound healing detection

The trauma area of each rat group was photographed and recorded on the day of DFU modeling, 3rd, 7th, 14th, and 21st days after modeling, respectively. By using a ruler as a standard, a fixed-height digital camera was utilized to photograph the trauma, with IPP 6.0 software to perform the measurement of trauma area and calculation of wound healing rate. Wound healing rate (%) = $(W_0\text{-}W)/W_0 \times 100\%$. W_0: original wound area of each group on DFU modeling day; W: wound area after modeling.

HE staining

We applied 4% paraformaldehyde to fix the traumatic tissues of each rat, which afterwards were paraffin-embedded, sectioned, and ultimately stained with hematoxylin (H3136, sigma) and eosin (E4009, sigma) for visualization of pathological structural changes of the traumatic tissues under a light microscope (Nikon Eclipse Ci-L, Nikon). Specific trauma tissue scores are presented below. Score 0: skin tissues are

essentially normal or have a large amount of neovascularization, with no significant inflammatory cell infiltration; Score 1: slight damage to skin tissues, with moderate amount of neovascularization and little inflammatory cell infiltration; Score 2: slight damaged skin tissues, with little neovascularization and little inflammatory cell infiltration; Score 3: moderate damaged skin tissues, with occasional neovascularization and medium inflammatory cell infiltration; Score 4: severe damage to skin tissues, and massive inflammatory cell infiltration.

ELISA

Following orbital blood sampling for each rat, the centrifugation was done and then obtain of the supernatant was performed. In accordance with instructions of Interleukin (IL)-6 ELISA kit (MM-0190R2, Meimian Industrial Co., Ltd.), IL-1β ELISA Kit (MM-0047R2, Meimian Industrial Co., Ltd.), Tumor necrosis factor-α (TNF-α) ELISA Kit (MM-0180R2, Meimian Industrial Co., Ltd.), rat Insulin (INS) ELISA Kit (CB10967-Ra, COIBO), rat Advanced Glycation End Products (AGEs) ELISA Kit (CB10818-Ra, COIBO), and rat receptor for Advanced Glycation End Products (RAGE) Kit (CB10819-Ra, COIBO), the estimation of IL-6, IL-1β, TNF-α, insulin (INS), AGEs and RAGE levels, namely absorbance values, were made at 450 nm.

Determination of oxidative stress levels

With collection of rat traumatic tissues, preparation of homogenate, centrifugation, and gain of supernatant were carried out. As per the step-by-step instructions of Total Superoxide Dismutase (T-SOD) Test Kit (A001-1, JIANCHENG BIOTECH), Reduced Glutathione (GSH) Content Test Kit (BC1175, Solarbio), Malondialdehyde (MDA) Determination Kit (A003-1, JIANCHENG BIOTECH), and Hydroxyproline (HYP) Content Test Kit (P0012, Beyotime), subsequent determination of SOD, GSH, MDA, and HYP content was conducted.

qRT-PCR

We employed RNA extraction kit (AG21024, Agbio) for total RNA from each rat traumatic tissues, and then synthesis of cDNA was done by reverse transcription kit (CW2569M, KangWei Co. Ltd.). Afterwards, SYBR Green qPCR kit (11201ES03, YiSheng Biotechnology Co. Ltd.) was employed to accomplish qRT-PCR. Quantification of IL-1β, IL-6, TNF-α, angiopoietins-1 (Ang-1), VEGF-c, and transmembrane receptor tyrosine kinase (Tie-2) mRNA expression was done by the $2^{-\Delta\Delta CT}$ assay. β-actin was taken as an internal reference gene. Primer sequence information was indicated below in Table 2.

Table 2
Primer sequence information

Gene	Forward Primer (5’-3’)	Reverse Primer (5’-3’)
Rat IL-1β	TGATGTTCCCATTCCACAGC	GAGGTGCTGATGTACCAGTT
Rat IL-6	TTCCAGCCAGTTGCCTTCTT	AGGTTTGCCGAGTAGACCTC
Rat TNF-α	AAGCCTGTAGCCCATGTTGT	CAGATAGATGGGCTCATACC
Rat Ang-1	GCTGGCAGTACAATGACAGT	GTATCTGGGCCATCTCCGAC
Rat VEGF-c	GCTTCTTGTCTCTGGCGTGT	TCCCGGATCACAATGCTTCA
Rat Tie-2	ATTGACGTGAAGATCAAGAATGCCACC	ATCCGGATTGTTTTTGGCCTTCCTGTT
Rat β-actin	GTCACCCACACTGTGCCCATCT	ACAGAGTACTTGCGCTCAGGAG
Notes:		

Abbreviations: TNF-α, Tumor necrosis factor-α; Ang-1, angiopoietins-1; VEGF-c, vascular endothelial growth factor-c; Tie-2, receptor tyrosine kinase.

Cell culture

Human dermal fibroblasts HDF-a cells (C0135C, Thermo Fisher) were cultured in human fibroblast expansion basal medium (M106500, Gibco) containing 10% FBS and 1% penicillin/streptomycin with 37°C, 70%-80% incubator humidity, and 5% CO_2. The observation of HDF-a cell morphology was made using a light microscope (AE2000, Motic).

Preparation of DSD-containing serum

Six normal rats were gavaged with the prepared 1.0 g/mL DSD solution at 9 a.m. and 4 p.m. for 7 d. An equal dose of saline were gavaged to another six normal rats. The collection of blood from the abdominal aorta 2 h after the last administration was carried out, with centrifugation at 4000 r/min for 15 min at 4°C so as to gain DSD-containing serum and normal serum. Following inactivation at 56°C for 30 min, filtration with 0.22 μm microporous filter membrane was performed to remove bacteria, kept at -80°C for spare parts.

CCK8 assay

Following inoculation of HDF-a cells into 24-well plates, intervention of DSD-containing serum at different concentrations (2.5%, 5%, 10%, 15%, 20%, 30%)[21][21] was constructed. After 24 h of incubation, assaying cell viability was done by CCK8 assay to select appropriate low, medium and high DSD-containing serum concentrations for subsequent experiments. Subsequently, the effects of different concentrations of DSD-containing serum in high glucose environment on HDF-a cell viability were examined for choosing optimal DSD-containing serum concentration.

Cell grouping

To confirm protective effects of DSD on HDF-a cells treated with high concentrations of glucose, these cells were randomized into control (Con) group, glucose (Glu27) group, Glu27 + blank drug-containing serum control (Blank) group, Glu27 + low concentration of DSD-containing serum (Low) group, Glu27 + medium concentration of DSD-containing serum (Medium) group, and Glu27 + high concentration of DSD-containing serum (High) group. Control cells received no treatment. The cells of Glu27 group were treated with 27 g/L glucose for 24 h[22][22]. Appropriate low, medium and high concentrations of DSD intervention for HDF-a cells with 27 g/L glucose treatment depended on results of CCK8 assay.

These HDF-a cells were randomly grouped into Blank group, Glu27 + optimal concentration of DSD-containing serum (DSD) group, Glu27 + LY2109761 (TGF-β pathway inhibitor, HY-12075, MCE, LY2109761) group, and Glu27 + optimal concentration of DSD-containing serum + LY2109761 (DSD + LY2109761) group. Cells in LY2109761 group were provided with 27 g/L glucose and 10 μM/L TGF-β pathway inhibitor, LY2109761, for 24 h incubation[23]. The DSD + LY2109761 group was intervened by 10 μM/L LY2109761 for 24 h after 27 g/L glucose treatment, with subsequent 24 h incubation with optimal concentration of DSD-containing serum. The determination of optimal concentration of DSD-containing serum was performed with results of CCK8 assay.

Cell scratching assay

In accordance with previous research method[22][22], photographs were obtained at 0 h and 24 h with a digital camera for recording the healing and scratch migration rate.

Flow cytometry

With collection of HDF-a cells for adjustment to 1×10^6/mL, addition of 500μL of binding buffer was carried out, with centrifugation and supernatant discarding. Then, 100μL of binding buffer, 5 μL of Annexin V-FITC and 10 μL of PI were added in order, well mixed. Light-avoidance reaction was done at room temperature for 15 min. Lastly, following addition of 400 μL of binding buffer, detection of apoptosis rate was made by flow cytometry within 1 h.

Western blot

After lysis of HDF-a cells completed by RIPA lysis buffer (P0013B, Beyotime), detection of total protein concentration was made by BCA kit (P0012, Beyotime). Following sequential SDS-PAGE electrophoresis, PVDF transmembrane and blocks, incubation with primary antibody (Table 3) was carried out overnight at 4°C, followed by incubation with secondary antibody (Table 3) at room temperature. The development and examination of protein bands were done by an ECL chemiluminescence meter (610020-9Q, Clinx).

Table 3
Antibody information for Western blot

Antibody	Company	Article Number
α-SMA Antibody	Affinity	BF9212
collagen I Antibody	Bioss	bs-10423R
AGEs Antibody	Bioss	bs-1158R
RAGE Antibody	Bioss	bs-0177R
TGF-β1 Antibody	Affinity	AF1027
Smad2 Antibody	Affinity	AF6449
p-smad2 Antibody	Affinity	AF3449
Smad3 Antibody	Affinity	AF6362
p-smad3 Antibody	Affinity	AF3362
Anti-rabbit IgG, HRP-linked Antibody	CST	7074
GAPDH Antibody	Proteintech	10494-1-AP
β-actin Antibody	Proteintech	81115-1-RR
Notes:		

Abbreviations: AGEs, advanced glycation end products; RAGE, receptor of advanced glycation endproducts.

Statistical analysis

Data analysis was conducted by SPSS statistical software (version 20.0, IBM). Measurement of data that met the tests for normal distribution and chi-square between multiple groups was made by one-way analysis of variance (ANOVA) method. The Turkey test was employed for two-by-two comparisons. For data that conformed to normal distribution with heterogeneous variance, Dunnett's T3 test or independent samples t-test was performed. Expression of all data was presented as mean ± standard deviation. A P value of less than 0.05 was defined as statistical significance.

Results

DSD intervention promoted wound healing in DFU rats

In Fig. 1A, there was worse wound healing occurred in DFU rats than in rats of Sham group, with significantly lower wound healing rate on days 3–21 ($P < 0.01$). On days 3 and 7, rats in the DM, DSD-M, and DSD-H groups exhibited increased wound healing rates than DFU rats ($P < 0.01$ or $P < 0.05$). On the 14th and 21st days, all DM and these different doses of DSD intervention led to greater wound closure (*P*

< 0.01). Furthermore, we employed HE staining to visualize the histopathological changes in the skin near trauma (Fig. 1B). The skin tissues of rats in Sham group remained basically normal, with no obvious damage and inflammatory cell infiltration. DFU modeling caused severely damaged skin tissues of rats, and severe necrosis of granulation tissue fibroblasts and capillaries, accompanied by a large number of inflammatory cell infiltration. Following both DM and DSD interventions, skin tissue damage in DFU rats were attenuated to varying degrees. The DFU rats remained significantly enhanced wound tissue scores than normal rats ($P < 0.01$). Wound tissue scores of DFU rats in the DM, DSD-M, and DSD-H groups exhibited reduced than those of rats in DFU group ($P < 0.01$ or $P < 0.05$).

DSD intervention caused reduced inflammatory response and oxidative stress levels, whereas promotion of angiogenesis in DFU rats

The determination of INS, IL-1β, IL-6, TNF-α, AGEs and RAGE levels in rat serum was made by ELISA assay (Fig. 2A-F). There were higher IL-1β, IL-6, TNF-α, AGEs and RAGE levels in DFU rats than in normal rats, whereas lowered INS levels ($P < 0.01$). It was observed that lower IL-1β, IL-6, TNF-α, AGEs and RAGE levels of DFU rats occurred in the DM, DSD-M, and DSD-H groups ($P < 0.01$). In addition, DFU rats in the DM, DSD-L, DSD-M, and DSD-H groups demonstrated elevated INS levels than in DFU group ($P < 0.01$).

We detected SOD, GSH, MDA, and HYP contents in rat traumatic tissue homogenates by biochemical kits (Fig. 2G-J). DFU rats exhibited reduced SOD, GSH, HYP contents, whereas elevated MDA content ($P < 0.01$). There was significantly higher SOD content in DFU rats of DM, DSD-M, and DSD-H groups than that of rats in DFU group ($P < 0.01$ or $P < 0.05$). Moreover, following DM and DSD treatment, we intuitively found increased GSH and HYP contents, with decreased MDA content ($P < 0.01$ or $P < 0.05$).

The IL-1β, IL-6, TNF-α, Ang-1, VEGF-c, and Tie-2 mRNA expression in traumatized rat tissues was examined by qRT-PCR assay, as displayed in Fig. 2K-P. DFU rats demonstrated elevated IL-1β, IL-6, and TNF-α mRNA expression, whereas lowered Ang-1, VEGF-c, and Tie-2 mRNA expression ($P < 0.01$). The DM, DSD-M, and DSD-H groups exhibited reduced IL-1β, IL-6, and TNF-α mRNA expression than those of DFU rats ($P < 0.01$ or $P < 0.05$), with higher Ang-1, VEGF-c, and Tie-2 mRNA expression ($P < 0.01$).

DSD intervention modulated TGF-β1, Smad2/3, AGE and RAGE protein expression to promote diabetic wound healing in DFU rats

Western blot assay was employed to measure TGF-β1, Smad2/3, p-Smad2/3, AGEs, and RAGE protein expression in rat trauma tissues (Fig. 3). There was decreased TGF-β1 and p-Smad3/Smad3 protein expression, whereas enhanced Smad2, p-Smad2/Smad2, AGEs, and RAGE expression occurred in DFU rats than in normal rats ($P < 0.01$ or $P < 0.05$). In contrast to DFU rats, TGF-β1 and p-Smad3/Smad3 protein levels in DM and DSD-H groups exhibited higher ($P < 0.01$ or $P < 0.05$), with lower Smad2, p-Smad2/Smad2, AGEs, and RAGE expression in DSD-M and DSD-H groups ($P < 0.01$ or $P < 0.05$). Additionally, DSD-L group demonstrated reduced Smad2 and p-Smad2/Smad2 protein expression, with elevated p-Smad3/Smad3 expression than DFU rats ($P < 0.01$ or $P < 0.05$).

DSD intervention facilitated HDF-a cell viability and migration with apoptosis inhibition under high glucose environments

The morphological observation of HDF-a cells was performed by a light microscopy, and we detected that HDF-a cells exhibited adherent growth with a flattened distribution of protruding spindle or star shapes (Fig. 4A). As displayed in Fig. 4B, the effects of DSD-containing serum under different concentrations (2.50%, 5.00%, 10.00%, 15.00%, 20.00%, and 30.00%) on HDF-a cell viability were detected by CCK8 assay. The cell viability in the 2.5% and 30% groups exhibited lower than that of control cells ($P < 0.01$ or $P < 0.05$). Therefore, we ultimately selected 10%, 15%, and 20% as the low, medium, and high concentrations of DSD-containing serum, respectively.

Subsequently, investigation of the effects of DSD-containing serum interventions with low, medium, and high concentrations on cell viability and migratory capacity in a high-glucose environment was carried out using CCK8 and cell scratch assays. In Fig. 4C, there was decreased cell viability in Glu27 group, Blank group, Low group (Glu27 + 10% concentration of DSD-containing serum), and Medium (Glu27 + 15% concentration of DSD-containing serum) group than in control group ($P < 0.01$). Moreover, cell migration rate of Glu27 group, Blank group, Low group, and Medium group demonstrated lowered than that of control cells, namely, a highly significantly reduced migratory ability (Fig. 4D, $P < 0.01$). The High (Glu27 + 20% concentration of DSD-containing serum) group underwent no no remarkable changes in cell viability and migration rate ($P > 0.05$). Depending on the above results, the optimal DSD-containing serum concentration was determined to be 20%, that is, the high concentration of DSD-containing serum intervention for subsequent studies.

We further performed the detection of changes in HDF-a cell migration capacity and viability in each group by cell scratch and CCK8 methods (Fig. 4E-F). There was enhanced cell migration rate, that is, increased migratory ability occurred in DSD (Glu27 + 20% of DSD-containing serum intervention) group whereas reduced migration rate in LY2109761 group than in Blank group (Fig. 4E, $P < 0.01$). The migration rate of HDF-a cells in DSD + LY2109761 group exhibited lower than in DSD group ($P < 0.01$). In addition, we intuitively observed increased cell viability in DSD group, with lowered HDF-a cell viability occurred in LY2109761 group than that of Blank group (Fig. 4F, $P < 0.01$). There was an decrease existed in DSD + LY2109761 group than in DSD group ($P < 0.01$). Flow cytometry assay to detect apoptosis rate of HDF-a cells was performed (Fig. 4G). The apoptosis rate demonstrated lower in DSD group, whereas higher in LY2109761 group than that of Blank group cells ($P < 0.01$). Following LY2109761 treatment, HDF-a cells intervened by 20% of DSD-containing serum exhibited an increased apoptosis rate ($P < 0.01$).

DSD intervention modulated TGF-β1, Smad2/3, AGE and RAGE protein expression to promote diabetic wound healing in HDF-a cells

Western blot assay was employed to measure α-SMA, collagen I, TGF-β1, Smad2/3, p-Smad2/3, AGEs, and RAGE protein expression in HDF-a cells (Fig. 5). In Fig. 4I-R, we visualized that a decrease on α-SMA,

collagen I, Smad2, AGEs, and RAGE protein expression ($P < 0.01$ or $P < 0.05$) and an increase on TGF-β1 and p-Smad3/Smad3 protein levels ($P < 0.01$) occurred in HDF-a cells with DSD treatment than in Blank group. There were reduced α-SMA, collagen I, Smad2, p-Smad2/Smad2, p-Smad3/Smad3, and AGEs protein levels in cells after LY2109761 intervention than those of cells in Blank group ($P < 0.01$ or $P < 0.05$). Following LY2109761 intervention, α-SMA, collagen I, p-Smad3/Smad3, AGEs, and RAGE protein levels in cells with 27 g/L glucose and 20% of DSD-containing serum intervention exhibited enhanced ($P < 0.01$ or $P < 0.05$), whereas lowered TGF-β1 and p-Smad2/Smad2 protein expression ($P < 0.01$).

Discussion

DFU, one of common diabetes complications of diabetes, remains an unaltered phenomenon with costly treatment, poor prognosis, major amputation risk and poor healing despite the current advances in wound healing methods[24]. Hence, search for more effective therapeutic strategies has become a priority. As a well-known classic formula, DSD has been applied for management of arthritis, diabetic peripheral neuropathy and coronary atherosclerotic heart disease[8][8]. A prior clinical study identified that DSD lowered AGEs levels of DFU patients to alleviate their symptoms[10]. However, there exists a paucity of studies relevant to the specific role and mechanisms of DSD in DFU treatment.

Reported essential pathophysiologic factors that contributed to delaying wound healing process included inflammatory response, elevated oxidative stress, delayed collagen synthesis, decreased angiogenesis, and dysfunction of fibroblasts and endothelial cells[25][25]. We observed that DSD intervention led to inhibit inflammatory factor expression to promote wound healing in DFU rats, in agreement with findings of Zhang *et al.* [26] [26] who applied San Huang Xiao Yan recipe to treat DFU. Ang-1 is capable of supporting the survival of neovascular endothelial cells as well as maintaining their stable state[27][27]. Tie-2, as Ang-1 receptor, upon binding to it, promotes angiogenesis as well as neovascularization maturation with further maintenance of vascular endothelial integrity[27][27]. As a cytokine, VEGF-c contributes to the survival, proliferation, and migration of endothelial cells, closely associated with angiogenesis[25][25]. Danggui Buxue decoction was identified to directly induce angiogenesis with enhancing VEGF, fibroblast growth factor-2, and Ang-1 expression[28][28]. Li *et al.* [25] [25] demonstrated that hesperidin treatment resulted in an increase in SOD and GSH levels, whereas a decrease in MDA and NO levels, while reversing down-regulation of VEGF-c, Ang-1, and Tie-2 expression occurred in wound tissues of DFU rats, in high accordance with our study. Furthermore, several studies have confirmed conclusively the role of AGEs-RAGE in DFU development[29, 30]. Hyperglycemia made induction of non-enzymatic glycosylation of proteins and lipids for AGEs formation, which, following binding to their receptor RAGE, further causing pro-inflammatory signaling and vascular endothelial damage, thereby delaying diabetic wound healing[30]. The application of ibrutinib by Yang *et al.* [29] [29] revealed that it led to lower RAGE, IL-1β, TNF-α, and IL-6 expression, whereas upregulated VEGF levels, which caused higher wound healing rate and wound healing promotion of DFU rats, matching findings of the present study. More importantly, a recent study has illustrated that DSD exerts its therapeutic effects on DFU primarily through AGE-RAGE pathway[15][15], further building solid theoretical foundation and scientific basis for our study.

Considered as one of the key cells in wound healing process, fibroblasts are implicated in the entire dynamic repair process, in addition to angiogenesis promotion[31]. Actually, hyperglycemia and AGEs are capable of directly inducing changes in fibroblasts, thereby contributing to epithelial dysfunction and delayed healing in diabetic wounds, which are mainly correlated with decreased fibroblast proliferation, increased apoptosis, and impaired migration to the wound site[32]. It was identified that Danggui Buxue decoction treatment directly induced angiogenesis with decreasd endothelial cell apoptosis[28][28]. Additionally, Wu *et al.* [22] [22] investigated mouse models and HDF-a cell models to demonstrate that Ruyi Jinhuang powder facilitated fibroblast proliferation and migration, with apoptosis inhibition, consequently accelerating diabetic wound healing, which maintained a high degree of consistency with results of the present study.

TGF-β, as a multifunctional bioactive cytokine, possesses regulatory functions in cell proliferation, migration, differentiation and apoptosis, whose induced α-SMA and collagen synthesis involved in tissue repair process of fibroblasts[33][33]. Smads proteins represent major downstream effector molecules in TGF-β signaling pathway[33][33]. It was found that TGF-β1 protein and mRNA expression levels exhibited reduced in serum of DFU patients[34]. Several studies have evidenced that herbal compounds or ingredients may facilitate DFU wound healing, with lowered oxidative stress and inflammatory cell infiltration amelioration with modulation of TGF-β1/Smads pathway[25, 35][25, 35]. Baicalin may be a key active ingredient in DSD treatment with findings of a network pharmacology investigation[36][36]. Mao *et al.*[37] detected that baicalin treatment enhanced mRNA expression of Ang-1, VEGF-c, TGF-β, Tie-2 and Smad2/3 in DFU rat tissues, improving inflammatory cell infiltration and angiogenesis, as well as decreasing MDA levels, potentially making it a candidate drug for DFU treatment. Moreover, Kang *et al.* [23] demonstrated that activation of TGF-β/Smad pathway caused promotion of wound healing in DFU mice, consistent with our findings. Meanwhile, we further performed TGF-β inhibitor intervention, LY2109761, to exhibit the important role of TGF-β pathway in DSD amelioration for DFU wound healing process. However, indeed, our study did not confirm in cellular experiments that DFU contributed to lower TGF-β1 and p-Smad3/Smad3 expression, and only validated this conclusion in the DFU rat model.

Conclusion

In conclusion, we demonstrated via *in vivo* and *in vitro* studies that DSD intervention may perform the inhibition of oxidative stress and inflammation levels, with promoting angiogenesis in DFU rats by regulating expression of AGEs/RAGE/TGF-β/Smad2/3, as well as lead to migration promotion and apoptosis suppression of fibroblasts to accelerate healing of DFU wounds, which offered a potential strategy for DFU treatment, and advanced the future of DSD clinical application for DFU.

Declarations

Acknowledgments

Not applicable.

Formatting of funding sources

This work was supported by the 2022 Shaoxing City Health Science and Technology Program [grant number 2022KY050].

Competing Interests Statement

The authors declare that they have no conflict of interest.

Authors' contributions

Conceptualization: [Shuyang Zhang]; Methodology: [Yanwen Xu]; Formal analysis and investigation: [Yanwen Xu], [Chenyang Zhang], [Jiayan Zhu], [Xiao Chen]; Writing-original draft preparation: [Yanwen Xu]; Writing-review and editing: [Shuyang Zhang]; Funding acquisition: [Shuyang Zhang]; Resources: [Xiao Chen]; Supervision: [Shuyang Zhang].

Data availability statement

All the data are contained in the manuscript.

Ethic approval

All animal experiments in this work were granted by the Animal Experimentation Ethics Committee of Zhejiang Eyong Pharmaceutical Research and Development Center (Certificate No. SYXK (Zhe) 2021-0033) and conducted following the guidelines of the Institutional Animal Care and Use Committee.

References

1. Huang F, Lu X, Yang Y, Yang Y, Li Y, Kuai L, Li B, Dong H, Shi J (2023) Microenvironment-Based Diabetic Foot Ulcer Nanomedicine. Adv Sci (Weinh) 10:e2203308. doi:10.1002/advs.202203308.
2. Armstrong DG, Tan TW, Boulton AJM, Bus SA (2023) Diabetic Foot Ulcers: A Review. Jama 330:62-75. doi:10.1001/jama.2023.10578.
3. Bonnet JB, Sultan A (2022) Narrative Review of the Relationship Between CKD and Diabetic Foot Ulcer. Kidney Int Rep 7:381-388. doi:10.1016/j.ekir.2021.12.018.
4. Zhou Q, Peng M, Zhou L, Bai J, Tong A, Liu M, Ng, Il, Cheng Y, Cai Y, Yang Y, Chen Y, Gao S, Li Z, Fu X, Shen M, Zhang J, Chen X (2018) Development and validation of a brief diabetic foot ulceration risk checklist among diabetic patients: a multicenter longitudinal study in China. Sci Rep 8:962. doi:10.1038/s41598-018-19268-3.
5. Wang Y, Wang C, Zheng L (2024) Bibliometric analysis of systematic review and meta-analysis on diabetic foot ulcer. Heliyon 10:e27534. doi:10.1016/j.heliyon.2024.e27534.
6. Li Y, Ren TT, Liu SS, Zhang L, Yi H, Li C, Chen LM, Gao HM, Yan LH, Liu XQ, Wang ZM (2024) Fingerprint analysis of dang-gui-Si-Ni decoction and its anticoagulant activity in vivo-in vitro. J

Ethnopharmacol 325:117890. doi:10.1016/j.jep.2024.117890.

7. Pan B, Wang Y, Wu C, Jia J, Huang C, Fang S, Liu L (2020) A Mechanism of Action Study on Danggui Sini Decoction to Discover Its Therapeutic Effect on Gastric Cancer. Front Pharmacol 11:592903. doi:10.3389/fphar.2020.592903.
8. Cheng B, Zheng H, Wu F, Wu J, Liu X, Tang C, Lu S, Chen Z, Song F, Ruan J, Zhang H, Song H, Liu W, Guo H, Liang Y, Su Z (2017) Metabolomics analysis of Danggui Sini decoction on treatment of collagen-induced arthritis in rats. J Chromatogr B Analyt Technol Biomed Life Sci 1061-1062:282-291. doi:10.1016/j.jchromb.2017.07.043.
9. Ding R, Wang Y, Zhu JP, Lu WG, Wei GL, Gu ZC, An ZT, Huo JG (2020) Danggui Sini decoction protects against oxaliplatin-induced peripheral neuropathy in rats. J Integr Neurosci 19:663-671. doi:10.31083/j.jin.2020.04.1154.
10. You WH, Wang P, Li MQ, Zhang Y, Peng YL, Zhang FL (2009) Therapeutic effects of modified Danggui Sini Decoction on plasma level of advanced glycation end products in patients with Wagner grade 0 diabetic foot: a randomized controlled trial. Zhong Xi Yi Jie He Xue Bao 7:622-628. doi:10.3736/jcim20090705.
11. Song J, Liu A, Liu B, Huang W, Jiang Z, Bai X, Hu L, Zheng S, Guo S, Wu J, Chen Q (2022) Natural Biologics Accelerate Healing of Diabetic Foot Ulcers by Regulating Oxidative Stress. Front Biosci (Landmark Ed) 27:285. doi:10.31083/j.fbl2710285.
12. Sun X, Wang X, Zhao Z, Chen J, Li C, Zhao G (2020) Paeoniflorin accelerates foot wound healing in diabetic rats though activating the Nrf2 pathway. Acta Histochem 122:151649. doi:10.1016/j.acthis.2020.151649.
13. Shi Y, Wang S, Zhang W, Zhu Y, Fan Z, Huang Y, Li F, Yang R (2022) Bone marrow mesenchymal stem cells facilitate diabetic wound healing through the restoration of epidermal cell autophagy via the HIF-1α/TGF-β1/SMAD pathway. Stem Cell Res Ther 13:314. doi:10.1186/s13287-022-02996-9.
14. Aljohi A, Matou-Nasri S, Liu D, Al-Khafaji N, Slevin M, Ahmed N (2018) Momordica charantia extracts protect against inhibition of endothelial angiogenesis by advanced glycation endproducts in vitro. Food Funct 9:5728-5739. doi:10.1039/c8fo00297e.
15. Ni X, Bao H, Guo J, Li D, Wang L, Zhang W, Sun G (2024) Discussion on the mechanism of Danggui Sini decoction in treating diabetic foot based on network pharmacology and molecular docking and verification of the curative effect by meta-analysis. Front Endocrinol (Lausanne) 15:1347021. doi:10.3389/fendo.2024.1347021.
16. Ye Z, Xian W, Ling GU, Zihang LI, Jingtian Z, Wenkai W, Liang Z, Mei X (2023) Efficacy of Danggui Buxue decoction on diabetic nephropathy-induced renal fibrosis in rats and possible mechanism. J Tradit Chin Med 43:507-513. doi:10.19852/j.cnki.jtcm.20230214.004.
17. Sun L, Yang Z, Zhao W, Chen Q, Bai H, Wang S, Yang L, Bi C, Shi Y, Liu Y (2022) Integrated lipidomics, transcriptomics and network pharmacology analysis to reveal the mechanisms of Danggui Buxue Decoction in the treatment of diabetic nephropathy in type 2 diabetes mellitus. J Ethnopharmacol 283:114699. doi:10.1016/j.jep.2021.114699.

18. Begum F, Manandhar S, Kumar G, Keni R, Sankhe R, Gurram PC, Beegum F, Teja MS, Nandakumar K, Shenoy RR (2023) Dehydrozingerone promotes healing of diabetic foot ulcers: a molecular insight. J Cell Commun Signal 17:673-688. doi:10.1007/s12079-022-00703-0.
19. Liu Y, Zhang X, Yang L, Zhou S, Li Y, Shen Y, Lu S, Zhou J, Liu Y (2023) Proteomics and transcriptomics explore the effect of mixture of herbal extract on diabetic wound healing process. Phytomedicine 116:154892. doi:10.1016/j.phymed.2023.154892.
20. Zhou H, Yang T, Lu Z, He X, Quan J, Liu S, Chen Y, Wu K, Cao H, Liu J, Yu L (2023) Liquiritin exhibits anti-acute lung injury activities through suppressing the JNK/Nur77/c-Jun pathway. Chin Med 18:35. doi:10.1186/s13020-023-00739-3.
21. Yang K, Bai Y, Yu N, Lu B, Han G, Yin C, Pang Z (2020) Huidouba Improved Podocyte Injury by Down-Regulating Nox4 Expression in Rats With Diabetic Nephropathy. Front Pharmacol 11:587995. doi:10.3389/fphar.2020.587995.
22. Wu M, Huang J, Shi J, Shi L, Zeng Q, Wang H (2022) Ruyi Jinhuang Powder accelerated diabetic ulcer wound healing by regulating Wnt/β-catenin signaling pathway of fibroblasts In Vivo and In Vitro. J Ethnopharmacol 293:115321. doi:10.1016/j.jep.2022.115321.
23. Geng K, Ma X, Jiang Z, Gu J, Huang W, Wang W, Xu Y, Xu Y (2023) WDR74 facilitates TGF-β/Smad pathway activation to promote M2 macrophage polarization and diabetic foot ulcer wound healing in mice. Cell Biol Toxicol 39:1577-1591. doi:10.1007/s10565-022-09748-8.
24. Rai V, Moellmer R, Agrawal DK (2022) Clinically relevant experimental rodent models of diabetic foot ulcer. Mol Cell Biochem 477:1239-1247. doi:10.1007/s11010-022-04372-w.
25. Li W, Kandhare AD, Mukherjee AA, Bodhankar SL (2018) Hesperidin, a plant flavonoid accelerated the cutaneous wound healing in streptozotocin-induced diabetic rats: Role of TGF-ß/Smads and Ang-1/Tie-2 signaling pathways. Excli j 17:399-419. doi:10.17179/excli2018-1036.
26. Zhang Z, Zheng Y, Chen N, Xu C, Deng J, Feng X, Liu W, Ma C, Chen J, Cai T, Xu Y, Wang S, Cao Y, Ge G, Jia C, Cao Y (2023) San Huang Xiao Yan recipe modulates the HMGB1-mediated abnormal inflammatory microenvironment and ameliorates diabetic foot by activating the AMPK/Nrf2 signalling pathway. Phytomedicine 118:154931. doi:10.1016/j.phymed.2023.154931.
27. Zhang MX, Huang XY, Song Y, Xu WL, Li YL, Li C (2022) Astragalus propinquus schischkin and Salvia miltiorrhiza bunge promote angiogenesis to treat myocardial ischemia via Ang-1/Tie-2/FAK pathway. Front Pharmacol 13:1103557. doi:10.3389/fphar.2022.1103557.
28. Dou Y, Shu Y, Wang Y, Jia D, Han Z, Shi B, Chen J, Yang J, Qin Z, Huang S (2023) Combination treatment of Danggui Buxue Decoction and endothelial progenitor cells can enhance angiogenesis in rats with focal cerebral ischemia and hyperlipidemia. J Ethnopharmacol 314:116563. doi:10.1016/j.jep.2023.116563.
29. Yang X, Cao Z, Wu P, Li Z (2019) Effect and Mechanism of the Bruton Tyrosine Kinase (Btk) Inhibitor Ibrutinib on Rat Model of Diabetic Foot Ulcers. Med Sci Monit 25:7951-7957. doi:10.12659/msm.916950.

30. Kang HJ, Kumar S, Dash BC, Hsia HC, Yarmush ML, Berthiaume F (2023) Multifunctional Elastin-Like Polypeptide Fusion Protein Coacervates Inhibit Receptor-Mediated Proinflammatory Signals and Promote Angiogenesis in Mouse Diabetic Wounds. Adv Wound Care (New Rochelle) 12:241-255. doi:10.1089/wound.2021.0102.
31. Addis R, Cruciani S, Santaniello S, Bellu E, Sarais G, Ventura C, Maioli M, Pintore G (2020) Fibroblast Proliferation and Migration in Wound Healing by Phytochemicals: Evidence for a Novel Synergic Outcome. Int J Med Sci 17:1030-1042. doi:10.7150/ijms.43986.
32. Deng H, Li B, Shen Q, Zhang C, Kuang L, Chen R, Wang S, Ma Z, Li G (2023) Mechanisms of diabetic foot ulceration: A review. J Diabetes 15:299-312. doi:10.1111/1753-0407.13372.
33. Zhang T, Wang XF, Wang ZC, Lou D, Fang QQ, Hu YY, Zhao WY, Zhang LY, Wu LH, Tan WQ (2020) Current potential therapeutic strategies targeting the TGF-β/Smad signaling pathway to attenuate keloid and hypertrophic scar formation. Biomed Pharmacother 129:110287. doi:10.1016/j.biopha.2020.110287.
34. Zhang F, Ren Y, Liu P, Ren Y, Wang D (2016) Expression of TGF-β1 and miRNA-145 in patients with diabetic foot ulcers. Exp Ther Med 11:2011-2014. doi:10.3892/etm.2016.3123.
35. Zhou X, Guo Y, Yang K, Liu P, Wang J (2022) The signaling pathways of traditional Chinese medicine in promoting diabetic wound healing. J Ethnopharmacol 282:114662. doi:10.1016/j.jep.2021.114662.
36. Feng C, Zhao M, Jiang L, Hu Z, Fan X (2021) Mechanism of Modified Danggui Sini Decoction for Knee Osteoarthritis Based on Network Pharmacology and Molecular Docking. Evid Based Complement Alternat Med 2021:6680637. doi:10.1155/2021/6680637.
37. Mao X, Li Z, Li B, Wang H (2021) Baicalin regulates mRNA expression of VEGF-c, Ang-1/Tie2, TGF-β and Smad2/3 to inhibit wound healing in streptozotocin-induced diabetic foot ulcer rats. J Biochem Mol Toxicol 35:e22893. doi:10.1002/jbt.22893.

Figures

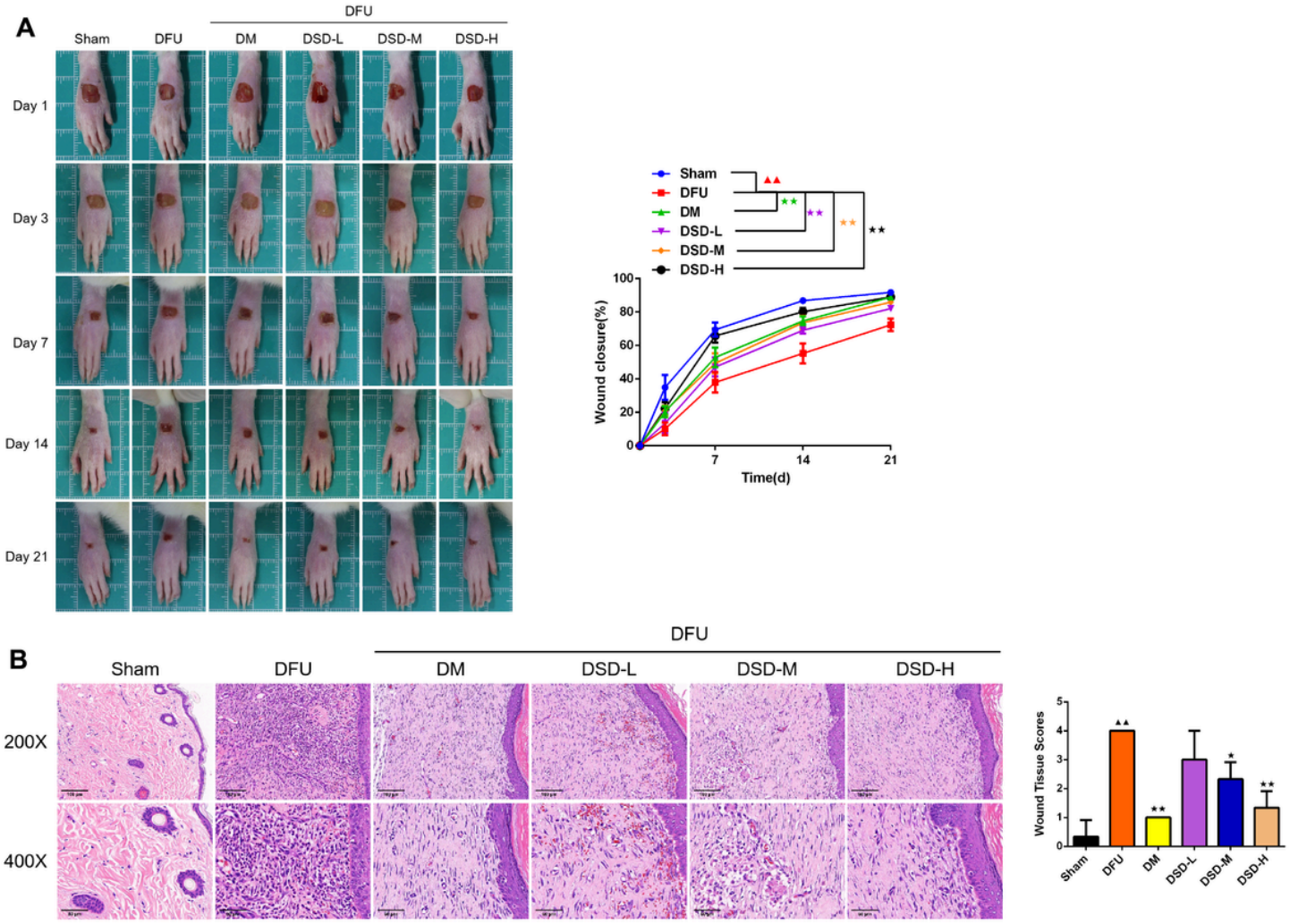

Figure 1

DSD intervention promoted wound healing in DFU rats

A: The observation of wound healing and calculation of wound closure were performed, *n*=6; B: We employed HE staining to visualize the histopathological changes in the skin near trauma (magnification 200×, scale bar: 100 μm; magnification 400×, scale bar: 50 μm), *n*=3; ▲*P*<0.05 and ▲▲*P*<0.01 vs. Sham group; □*P*<0.05 and □□*P*<0.01 vs. DFU group; **Note**: DFU: diabetic foot ulcer; DM: metformin; DSD: Dang-Gui-Si-Ni.

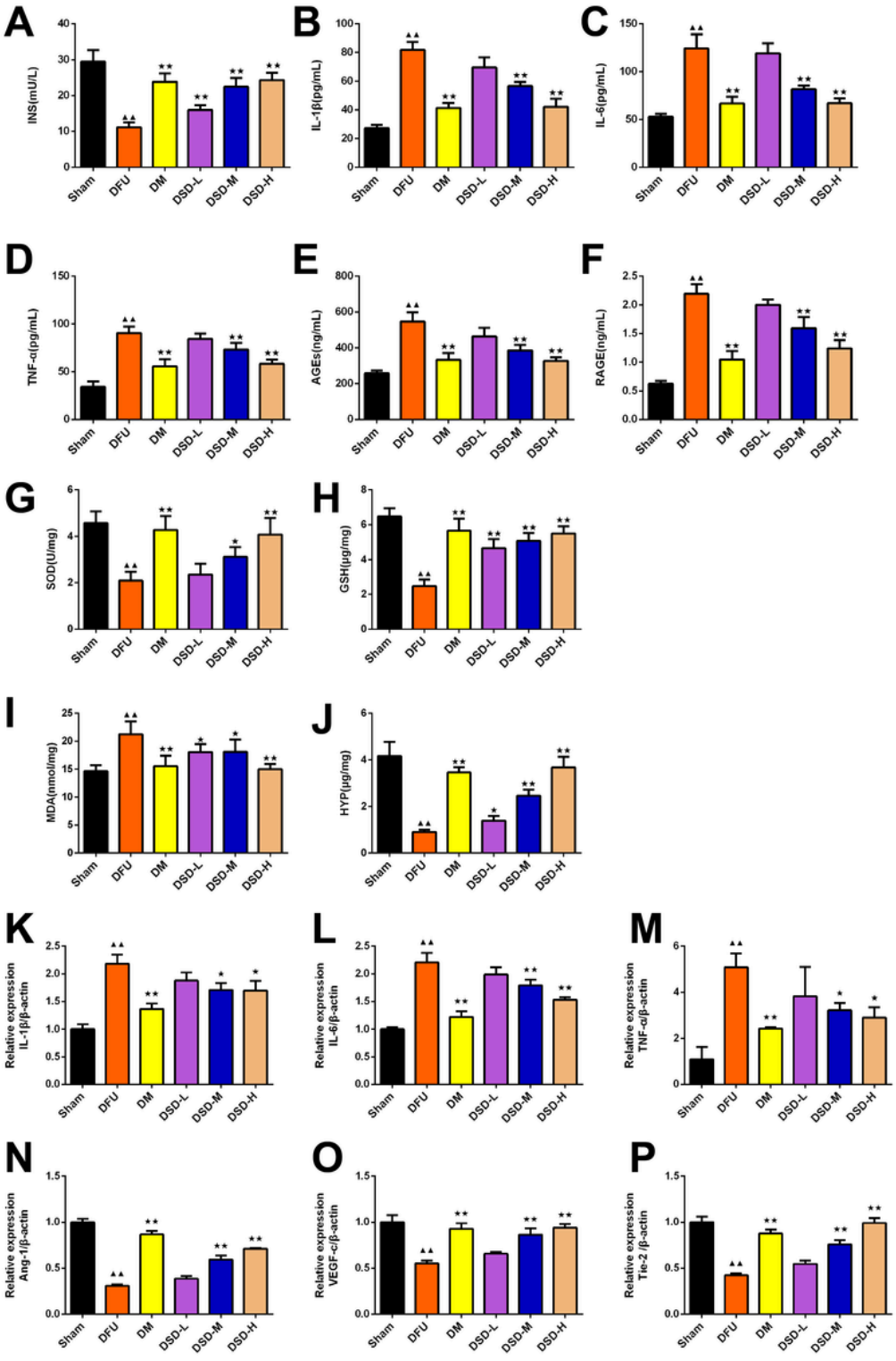

Figure 2

DSD intervention caused reduced inflammatory response and oxidative stress levels, whereas promotion of angiogenesis in DFU rats

The determination of INS (A), IL-1β (B), IL-6 (C), TNF-α (D), AGEs (E) and RAGE (F) levels in rat serum was made by ELISA assay, *n*=6; We detected SOD (G), GSH (H), MDA (I), and HYP (J) contents in rat traumatic

tissue homogenates by biochemical kits, *n*=6; The IL-1β (K), IL-6 (L), TNF-α (M), Ang-1 (N), VEGF-c (O), and Tie-2 (P) mRNA expression in traumatized rat tissues was examined by qRT-PCR assay, *n*=3; ▲*P*<0.05 and ▲▲*P*<0.01 vs. Sham group; □*P*<0.05 and □□*P*<0.01 vs. DFU group; **Note**: DFU: diabetic foot ulcer; DM: metformin; DSD: Dang-Gui-Si-Ni; INS: insulin; AGEs: advanced glycation end products; RAGE: receptor of advanced glycation endproducts; SOD: Superoxide dismutase; GSH: glutathione; MDA: malondialdehyde; HYP: hydroxyproline; Ang-1: angiopoietins-1; VEGF-c: vascular endothelial growth factor-c; Tie-2: transmembrane receptor tyrosine kinase.

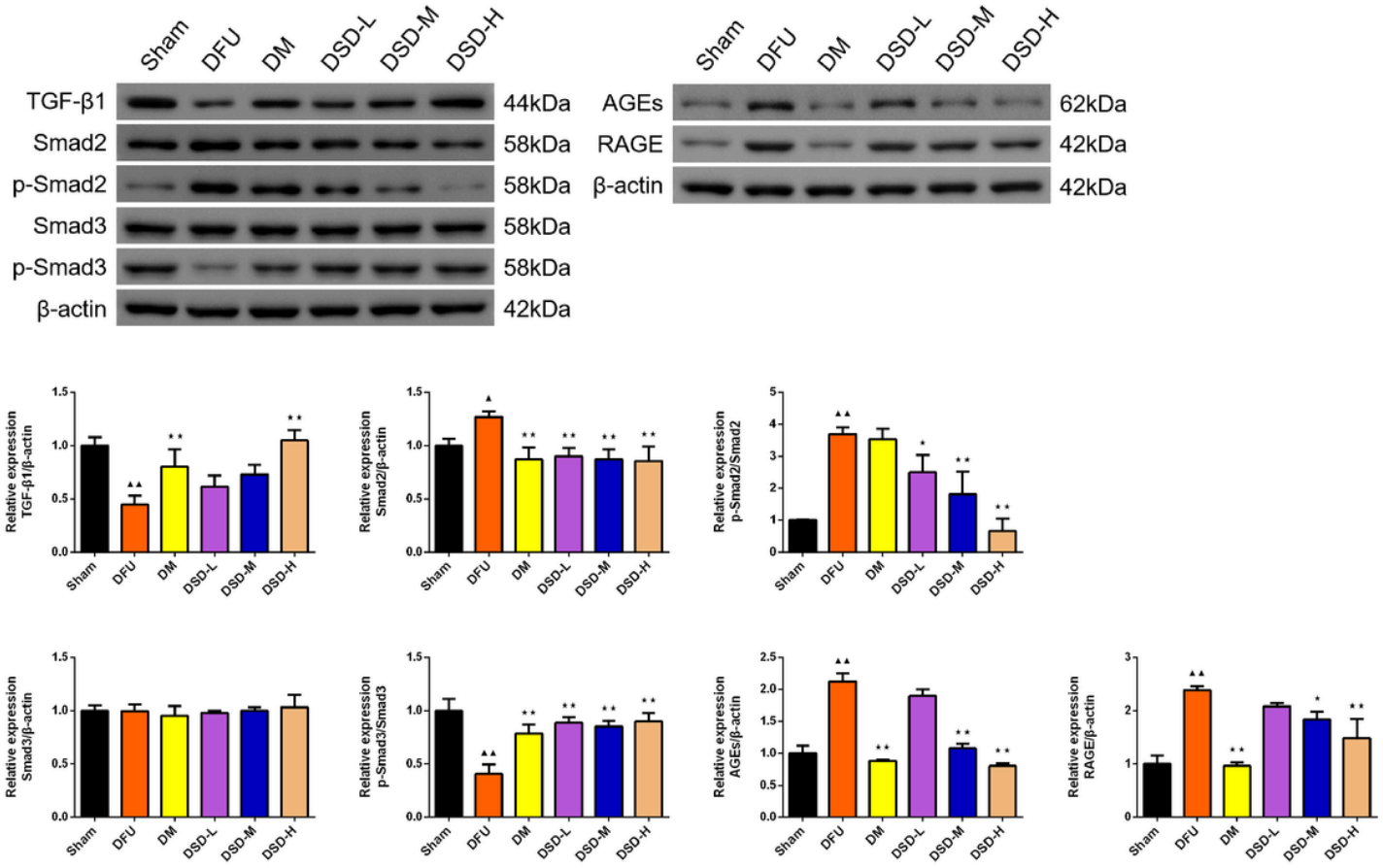

Figure 3

DSD intervention modulated TGF-β1, Smad2/3, AGE and RAGE protein expression to promote diabetic wound healing in DFU rats

Western blot assay was employed to measure TGF-β1, Smad2, p-Smad2/Smad2, Smad3, p-Smad3/Smad3, AGEs, and RAGE protein expression in rat trauma tissues, *n*=3; ▲*P*<0.05 and ▲▲*P*<0.01 vs. Sham group; □*P*<0.05 and □□*P*<0.01 vs. DFU group; **Note**: DFU: diabetic foot ulcer; DSD: Dang-Gui-Si-Ni; DM: metformin; AGEs: advanced glycation end products; RAGE: receptor of advanced glycation endproducts.

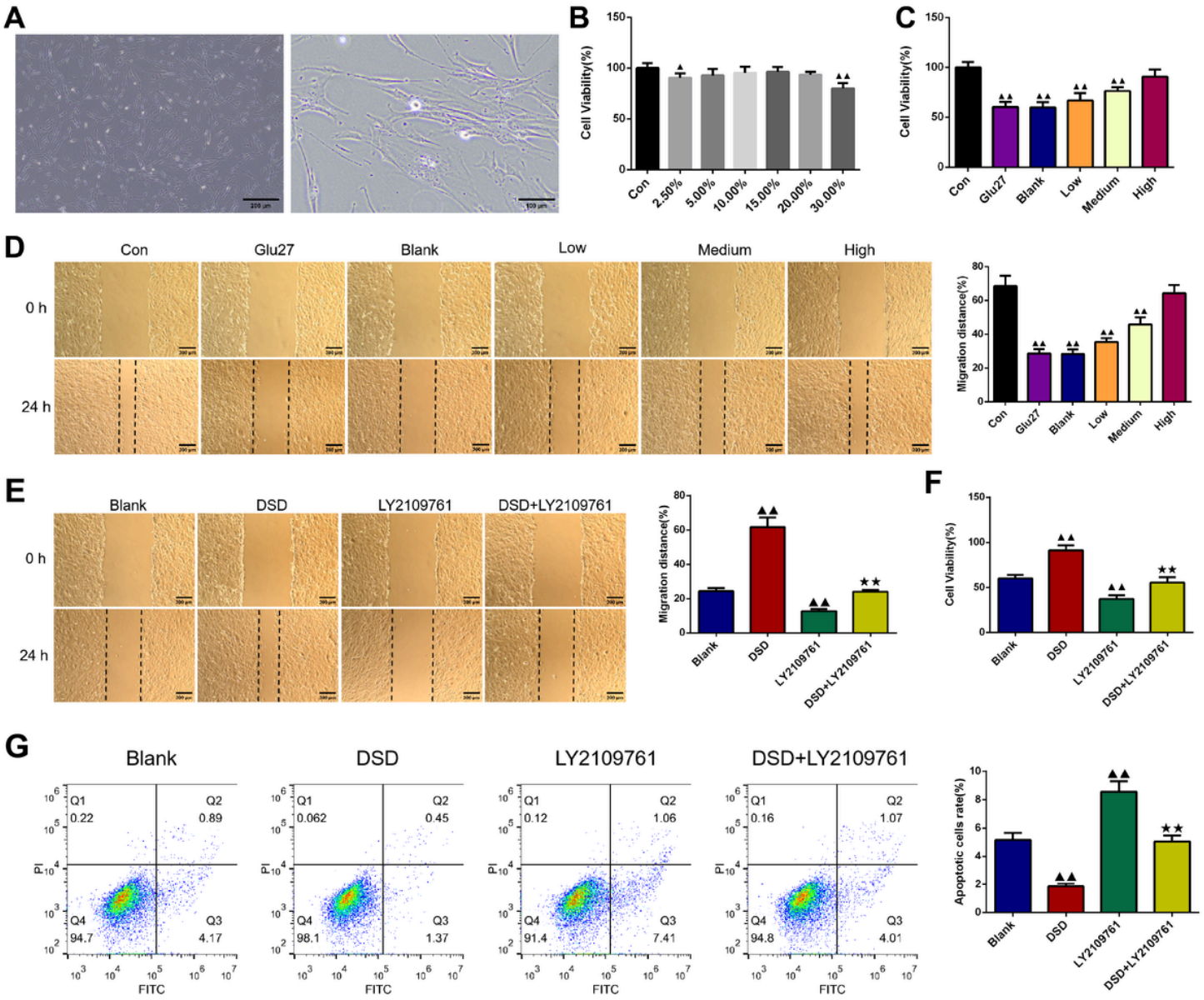

Figure 4

DSD intervention facilitated HDF-a cell viability and migration with apoptosis inhibition under high glucose environments

A: The morphological observation of HDF-a cells was performed by a light microscopy (magnification 100×, scale bar: 200 μm; magnification 200×, scale bar: 100 μm); B: The effects of DSD-containing serum under different concentrations (2.50%, 5.00%, 10.00%, 15.00%, 20.00%, and 30.00%) on HDF-a cell viability were detected by CCK8 assay, n=6, ▲P<0.05 and ▲▲P<0.01 vs. Con group; The investigation of effects of DSD-containing serum interventions with low, medium, and high concentrations on cell viability and migratory capacity in a high-glucose environment was carried out using CCK8 (C) and cell scratch (D) assays (magnification 40×, scale bar: 300 μm), n=6, ▲P<0.05 and ▲▲P<0.01 vs. Con group; We further performed detection of changes in HDF-a cell migration capacity and viability in each group by cell scratch (E, magnification 40×, scale bar: 300 μm) and CCK8 (F) methods, n=6; G: Flow cytometry assay

to detect apoptosis rate of HDF-a cells was performed, *n*=3; ▲*P*<0.05 and ▲▲*P*<0.01 vs. Blank group; □*P*<0.05 and □□*P*<0.01 vs. DSD group; Note: Con: control; Glu27: cells with 27 g/L glucose; Blank: cells with 27 g/L glucose and normal serum intervention; Low: cells with 27 g/L glucose and 10% of DSD-containing serum intervention; Medium: cells with 27 g/L glucose and 15% of DSD-containing serum intervention; High: cells with 27 g/L glucose and 20% of DSD-containing serum intervention; DSD: cells with 27 g/L glucose and 20% of DSD-containing serum intervention; LY2109761: cells with 27 g/L glucose and 10 μM/L TGF-β pathway inhibitor, LY2109761, for 24 h incubation; DSD + LY2109761: cells with 27 g/L glucose, 20% of DSD-containing serum intervention and 10 μM/L LY2109761 for 24 h incubation.

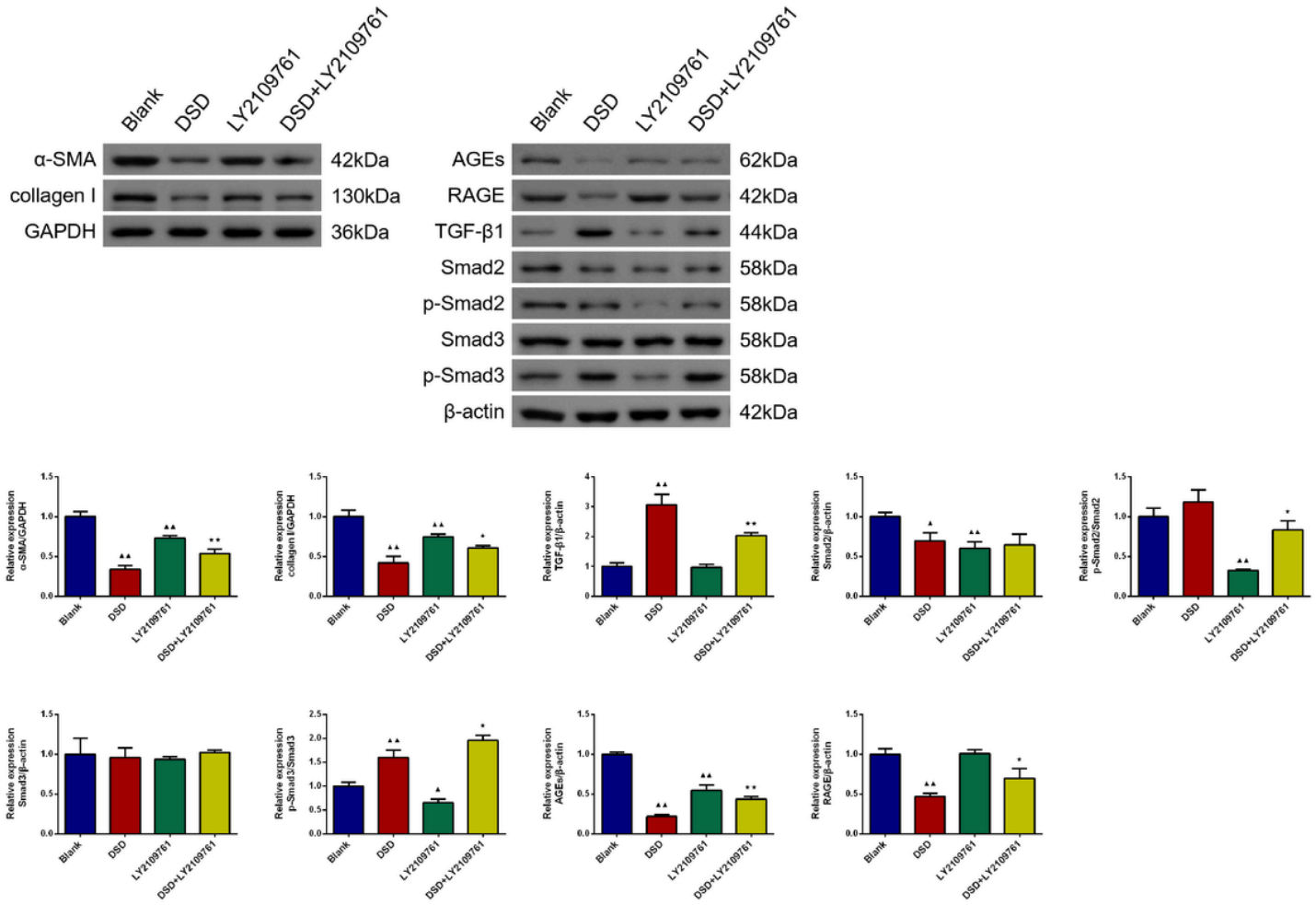

Figure 5

DSD intervention modulated TGF-β1, Smad2/3, AGE and RAGE protein expression to promote diabetic wound healing in HDF-a cells

The measurement of α-SMA, collagen I, TGF-β1, Smad2, p-Smad2/Smad2, Smad3, p-Smad3/Smad3, AGEs, and RAGE protein expression was made by Western blot assay in HDF-a cells, *n*=3; ▲*P*<0.05 and ▲▲*P*<0.01 vs. Blank group; □*P*<0.05 and □□*P*<0.01 vs. DSD group; **Note**: AGEs: advanced glycation end

products; RAGE: receptor of advanced glycation endproducts; α-SMA: α-smooth muscle actin; Blank: cells with 27 g/L glucose and normal serum intervention; DSD: cells with 27 g/L glucose and 20% of DSD-containing serum intervention; LY2109761: cells with 27 g/L glucose and 10 μM/L TGF-β pathway inhibitor, LY2109761, for 24 h incubation; DSD + LY2109761: cells with 27 g/L glucose, 20% of DSD-containing serum intervention and 10 μM/L LY2109761 for 24 h incubation.